In-field critical current of type-II superconductors caused by strain from nanoscale columnar inclusions

J. P. Rodriguez,[1] P. N. Barnes,[2] and C. V. Varanasi[3]
[1]*Department of Physics and Astronomy, California State University, Los Angeles, California 90032, USA*
[2]*Air Force Research Laboratory, Wright-Patterson Air Force Base, Dayton, Ohio 45433, USA*
[3]*University of Dayton Research Institute, Dayton, Ohio 45469, USA*
(Received 2 April 2008; revised manuscript received 17 June 2008; published 18 August 2008)

The results of a linear elasticity analysis yields that nanorod inclusions aligned along the *c* axis of a thin film of $YBa_2Cu_3O_{7-\delta}$, such as $BaZrO_3$ and $BaSnO_3$, squeeze that matrix by pure shear. The sensitivity of the superconducting critical temperature in that material to the latter implies that the phase boundary separating the nanorod inclusion from the superconductor acts as a collective pinning center for the vortex lattice that appears in external magnetic field. A dominant contribution to the in-field critical current can result. The elasticity analysis also yields that the growth of nanorod inclusions can be weakly metastable when the inclusion is softer than the matrix.

DOI: 10.1103/PhysRevB.78.052505 PACS number(s): 74.25.Qt, 62.20.D−, 74.25.Sv, 68.35.Gy

I. INTRODUCTION

The ongoing development of thin films of superconducting $YBa_2Cu_3O_{7-\delta}$ (YBCO) for wire technology has resulted in world record high critical currents.[1] In external magnetic field, the critical current is considerably enhanced by nanorod inclusions that are aligned in parallel to the crystalline *c* axis.[2–5] The enhancement is strongest at orientations of the magnetic field parallel to the *c* axis. Understanding the fundamental physics behind this effect remains a challenge. It is also unknown what drives the growth of nanorods in the first place in YBCO films.

In this Brief Report, we provide insight into both of these questions by computing the strain field due to nanorod inclusions that thread a YBCO superconductor along the *c* axis. The lattice constant of inclusions that optimize the critical current is typically 8% larger than that of the YBCO matrix in the *a-b* plane. Assuming a coherent phase boundary between the inclusion and a given epitaxial layer of YBCO, a linear elasticity analysis yields that the nanocolumn is compressed axially, while the YBCO matrix is squeezed by pure shear about the nanocolumn. The critical temperature in optimally doped YBCO is known to couple strongly to pure shear in the *a-b* plane.[6] In applied magnetic field, we show theoretically how this experimental fact results in substantial collective pinning of the vortex lattice by the phase boundary separating the nanocolumn inclusion from the YBCO matrix.[7,8] Also, the elastic energy shows weak metastability at a high density of nanocolumns when the nanocolumn is soft compared to the YBCO layer (see Fig. 1). We believe that this drives epitaxial growth of nanorod inclusions in YBCO films.

II. TWO-DIMENSIONAL ELASTICITY THEORY

We shall determine first the elastic strain and the elastic energy cost due to a single nanorod inclusion that threads a film of YBCO along the *c* axis. Such nanorods are typically composed either of $BaZrO_3$ (BZO) (Ref. 2 and 3) or of $BaSnO_3$ (BSO).[4] Both are cubic perovskites, with lattice constants (a_{in}) that exceed that of the *a-b* plane in YBCO, $a_{out}=3.86$ Å, by 9% and by 7%, respectively.[2–4] Let us temporarily ignore the effect of the lattice mismatch along the *c* axis by considering only epitaxial layers that are far from any possible partial misfit dislocation and that therefore present a coherent phase boundary between the inclusion and the YBCO matrix. Such partial misfit dislocations are accompanied by stacking faults,[9] a topic which will be discussed later in the concluding section. The assumption of a coherent phase boundary is valid for a nanorod inclusion of diameter less than the distance between possible misfit dislocations,[9] $a_{Moire}=(a_{out}^{-1}-a_{in}^{-1})^{-1}$. BZO nanorods typically have a diameter of[3] 2–3 nm, which satisfies the bound $a_{Moire}=5$ nm. BSO nanocolumns, on the other hand, typically have a diameter of[4] 7–8 nm. It exceeds $a_{Moire}=6$ nm, although not by much.

Consider then a cylindrical nanocolumn inclusion that presents a coherent phase boundary with a given epitaxial layer of the YBCO matrix. Unit cells match up one to one across the phase boundary in such case. The ideal axial sym-

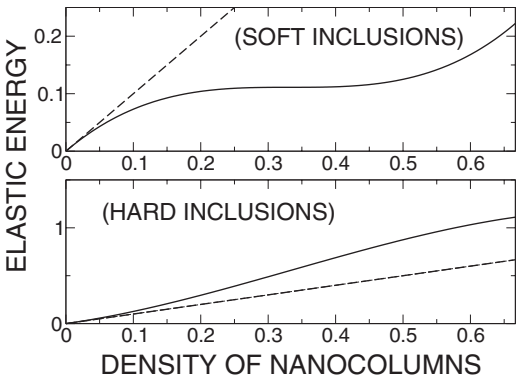

FIG. 1. The total elastic energy density Eq. (13), in units of $E_{2D}^{(1)}/\pi r_1^2$, versus the density of nanocolumn inclusions, in units of $1/\pi r_1^2$, is plotted. The dashed line above corresponds to the elastic energy of isolated nanocolumn inclusions. The radii in Eq. (13) are set to $r_2^2=\pm 3r_1^2$ for relatively soft and hard nanocolumns, respectively.

metry, assumed here for simplicity, implies a radial displacement field, $\mathbf{u}(\mathbf{r})=u(r)\hat{\mathbf{r}}$. We then have the boundary condition,

$$u_{\text{out}}(r_{\text{out}})-u_{\text{in}}(r_{\text{in}})=r_{\text{in}}-r_{\text{out}}, \tag{1}$$

between the displacement fields of the nanocolumn (in) and of the YBCO layer (out) at the phase boundary. The in-plane lattice mismatch that it represents generates elastic strain in both the inclusion and in the YBCO matrix. The elastic energy due to a two-dimensional (2D) strain field is given by the integral,[9]

$$E_{\text{2D}}=\int' d^2r\left\{\frac{1}{2}c_{\parallel}(\nabla\cdot\mathbf{u})^2+\frac{1}{2}c_{\perp}\left[\left(\frac{\partial u_x}{\partial x}-\frac{\partial u_y}{\partial y}\right)^2+\left(\frac{\partial u_x}{\partial y}+\frac{\partial u_y}{\partial x}\right)^2\right]\right\}, \tag{2}$$

over the corresponding area (prime), which is confined to $r<r_{\text{in}}$ for the nanocolumn and to $r>r_{\text{out}}$ for the YBCO matrix. Here, $c_{\parallel}$ and $c_{\perp}$ are the 2D bulk compression and the 2D shear moduli, respectively. A useful identity for the pure shear component above reads

$$\left(\frac{\partial u_x}{\partial x}-\frac{\partial u_y}{\partial y}\right)^2+\left(\frac{\partial u_x}{\partial y}+\frac{\partial u_y}{\partial x}\right)^2=2(\nabla\mathbf{u})^2-(\nabla\cdot\mathbf{u})^2-(\nabla\times\mathbf{u})^2. \tag{3}$$

The strain tensor takes the form $\nabla\mathbf{u}=(du/dr)\hat{\mathbf{r}}\hat{\mathbf{r}}+(u/r)\hat{\boldsymbol{\phi}}\hat{\boldsymbol{\phi}}$ in the present axially symmetric case. Combined with Eq. (3), it results in the compact expression for the elastic energy, $E_{\text{2D}}=\int d^2r\{\frac{1}{2}c_{\parallel}[r^{-1}d(ru)/dr]^2+\frac{1}{2}c_{\perp}[rd(r^{-1}u)/dr]^2\}$. Calculus of variations then yields a nanocolumn inclusion squeezed by pure compression and a surrounding YBCO matrix squeezed by pure shear,

$$u_{\parallel}(r)=-A_0r \quad \text{for} \quad r<r_{\text{in}}, \quad \text{and} \quad u_{\perp}(r)=+B_0r_{\text{out}}^2/r \quad \text{for} \quad r>r_{\text{out}}, \tag{4}$$

with corresponding strain tensors,

$$\nabla\mathbf{u}_{\parallel}=-A_0\mathbf{I} \quad \text{and} \quad \nabla\mathbf{u}_{\perp}=B_0(r_{\text{out}}/r)^2(\hat{\boldsymbol{\phi}}\hat{\boldsymbol{\phi}}-\hat{\mathbf{r}}\hat{\mathbf{r}}). \tag{5}$$

The total elastic energy Eq. (2) generated by the nanocolumn inclusion is then $E_{\text{2D}}^{(1)}=2c_{\parallel}^{(\text{in})}\pi r_{\text{in}}^2A_0^2+2c_{\perp}^{(\text{out})}\pi r_{\text{out}}^2B_0^2$. Minimizing it with respect to the constants A_0 and B_0 while enforcing the boundary condition, Eq. (1) yields optimal values $r_{\text{in}}A_0=(\Delta r)c_{\perp}^{(\text{out})}/[c_{\parallel}^{(\text{in})}+c_{\perp}^{(\text{out})}]$ and $r_{\text{out}}B_0=(\Delta r)c_{\parallel}^{(\text{in})}/[c_{\parallel}^{(\text{in})}+c_{\perp}^{(\text{out})}]$. Here $\Delta r=r_{\text{in}}-r_{\text{out}}$. These then yield an elastic energy cost,

$$E_{\text{2D}}^{(1)}=2\pi(\Delta r)^2[c_{\parallel}^{(\text{in})-1}+c_{\perp}^{(\text{out})-1}]^{-1}, \tag{6}$$

for the nanocolumn inclusion, which has an equilibrium radius $r_{\text{out}}+u_{\text{out}}(r_{\text{out}})$ given by $r_0=[c_{\parallel}^{(\text{in})}r_{\text{in}}+c_{\perp}^{(\text{out})}r_{\text{out}}]/[c_{\parallel}^{(\text{in})}+c_{\perp}^{(\text{out})}]$.

Let us consider next a field of many cylindrical nanocolumn inclusions of radius r_0 centered at transverse locations $\{\mathbf{R}_n\}$. Suppose again that they all present a coherent phase boundary with a given epitaxial layer of the YBCO matrix. The displacement field is then a linear superposition of those generated by a single nanocolumn inclusion Eq. (4);

$$\mathbf{u}_{\text{in}}(\mathbf{r})=\mathbf{u}_{\parallel}(\mathbf{r}-\mathbf{R}_i)+\sum_{j\neq i}\mathbf{u}_{\perp}[(r_{\text{out}}/r_{\text{in}})(\mathbf{r}-\mathbf{R}_i)+\mathbf{R}_i-\mathbf{R}_j], \tag{7}$$

inside the ith nanocolumn and

$$\mathbf{u}_{\text{out}}(\mathbf{r})=\sum_j\mathbf{u}_{\perp}(\mathbf{r}-\mathbf{R}_j), \tag{8}$$

inside the YBCO matrix. The pure shear terms that have been added to the pure compression inside of a nanocolumn Eq. (7) are required by the boundary condition Eq. (1). Observe now, by Eq. (5), that $\nabla^2\mathbf{u}_{\parallel}=0=\nabla^2\mathbf{u}_{\perp}$. Inspection of the elastic energy functional Eq. (2) combined with the identity Eq. (3) then yields that the above superpositions are stationary because $\nabla\cdot\mathbf{u}_{\perp}$, $\nabla\times\mathbf{u}_{\parallel}$, and $\nabla\times\mathbf{u}_{\perp}$ all vanish. Indeed, the elastic energy cost reduces to a sum of surface integrals around the phase boundaries of the form $E_{\text{2D}}=\Sigma_iE_{\text{2D}}^{(1)}+\Sigma_i\Sigma_j'[e_{i,j,i}(\text{out})+e_{i,i,j}(\text{out})]+\Sigma_i\Sigma_{j,k}'[e_{i,j,k}(\text{in})+e_{i,j,k}(\text{out})]$, where the indices j and k refer to the terms in the superpositions Eqs. (7) and (8) and where the index i refers to the phase boundary. The prime notation over the summation symbols indicates that $i\neq j,k$. Each individual contribution $e_{i,j,k}$ is given by a surface integral around the circle S_i of radius r_{out} that is centered at $\mathbf{R}_i$: $e_{i,j,k}(X)=\text{sgn}(X)c_{\perp}^{(X)}I_{i,j,k}$, with

$$I_{i,j,k}=\oint_{S_i}d\mathbf{a}\cdot[\nabla\mathbf{u}_{\perp}(\mathbf{r}-\mathbf{R}_j)]\cdot\mathbf{u}_{\perp}(\mathbf{r}-\mathbf{R}_k). \tag{9}$$

Here, $\text{sgn}(\text{in})=+1$ and $\text{sgn}(\text{out})=-1$. Also, the measure $d\mathbf{a}$ on the circle S_i points radially outward. Substituting in the strain fields Eq. (5) above yields ultimately that $e_{i,j,i}=0=e_{i,i,j}$ and that

$$e_{i,j,k}(X)=\text{sgn}(X)c_{\perp}^{(X)}(2\pi)B_0^2r_{\text{out}}^6\,\text{Re}[R_{i,j}R_{i,k}e^{i\phi_{j,k}(i)}-r_{\text{out}}^2]^{-2}, \tag{10}$$

for $i\neq j,k$ (see Appendix). Here, $\mathbf{R}_{i,j}=\mathbf{R}_i-\mathbf{R}_j$, and $\phi_{j,k}(i)$ denotes the angle between the vectors $\mathbf{R}_{i,j}$ and $\mathbf{R}_{i,k}$. The 2D elastic energy then is composed of a sum of one-body, two-body ($j=k$) and three-body terms ($j\neq k$), $E_{\text{2D}}=\Sigma_iE_{\text{2D}}^{(1)}+\Sigma_i\Sigma_{j,k}'V_{i,j,k}$, with the interaction energy given by

$$V_{i,j,k}=-(2\pi)[c_{\perp}^{(\text{out})}-c_{\perp}^{(\text{in})}]B_0^2r_{\text{out}}^6\,\text{Re}[R_{i,j}R_{i,k}e^{i\phi_{j,k}(i)}-r_{\text{out}}^2]^{-2}. \tag{11}$$

Notice that $V_{i,j,k}$ changes sign as a function of the relative rigidity between the nanocolumn inclusion and the YBCO matrix.

The elastic energy will now be obtained by computing subsequent self-energy corrections to the two-body interaction and to the one-body line tension. Let us first fix the coordinate for the phase boundary above, $\mathbf{R}_i$, as well as one of the nanocolumn coordinates above, $\mathbf{R}_j$. Observe that the three-body interaction Eq. (11) has zero angle average about the center $\mathbf{R}_i$ over the remaining nanocolumn coordinate $\mathbf{R}_k$. This is due simply to the fact that the contour integral $\oint dzz^{-1}(z-w)^{-2}$ around the unit circle, $z=\exp[i\phi_{j,k}(i)]$, vanishes for complex w inside that circle. Let us assume that each nanocolumn has a hard core of radius $r_1\sim r_0$. At $R_{i,j}$

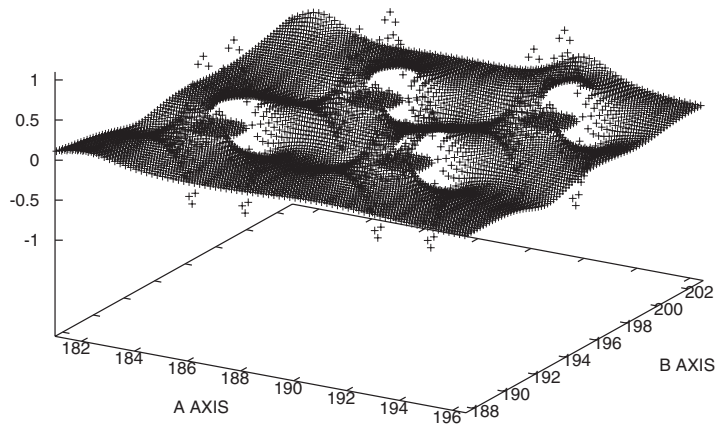

FIG. 2. A potential-energy landscape for a single vortex line in units of $|\varepsilon_p|$ and the coherence length that results from a superposition of 2744 d-wave collective pinning centers [Eq. (14)] arranged in a "liquid" fashion is displayed (see Ref. 8).

$\gg r_1$, we then obtain the estimate $\Sigma_k' V_{i,j,k} = -\pi r_1^2 n_\phi V_{i,j,j}$ for the correction to the two-body interaction on average over the bulk of the system. Here, n_ϕ denotes the density of nanocolumns. The renormalized two-body interaction that results is then $V_{i,j}^{(2)} = (1 - \pi r_1^2 n_\phi) V_{i,j,j}$. Next, let us assume an effective hard core of radius $r_2' \sim r_1$ for the nanocolumn at the coordinate $\mathbf{R}_j$ that remains. We thereby obtain the estimate $\Sigma_{j,k}' V_{i,j,k} = n_\phi \int' d^2 R_{i,j} V_{i,j}^{(2)} = -\pi r_2^2 n_\phi (1 - \pi r_1^2 n_\phi) E_{2D}^{(1)}$ for the net self-energy correction to the elastic energy of an isolated nanocolumn inclusion, with

$$r_2^2 = \{[1 - c_\perp^{(\mathrm{in})}/c_\perp^{(\mathrm{out})}]/[1 + c_\perp^{(\mathrm{out})}/c_\parallel^{(\mathrm{in})}]\} \cdot [r_{\mathrm{out}}^4/(r_2'^2 - r_{\mathrm{out}}^2)]. \tag{12}$$

This yields a total elastic energy density,

$$E_{2D}/A = [1 - \pi r_2^2 n_\phi (1 - \pi r_1^2 n_\phi)] n_\phi E_{2D}^{(1)}, \tag{13}$$

as a function of the density of nanocolumns. The above third-order polynomial is depicted by Fig. 1. It notably predicts weakly metastable epitaxial growth for relatively soft nanorods within the YBCO matrix, such that $c_\perp^{(\mathrm{in})} < c_\perp^{(\mathrm{out})}$. This occurs at a density $n_\phi = \{1 + [1 - (3r_1^2/r_2^2)]^{1/2}\}/3\pi r_1^2$ of nanorod inclusions at large effective cross sections $\pi r_2^2 > 3\pi r_1^2$. The equilibrium density of nanorod inclusions therefore *cannot* be diluted. In particular, the effective volume fraction $\pi r_1^2 n_\phi$ must lie somewhere between 1/3 and 2/3. An inspection of Eq. (12) indicates that the former condition requires some degree of agglomeration among the nanocolumn inclusions; $r_{\mathrm{out}} < r_2' < 2 r_{\mathrm{out}}$. This may, however, be an artifact of the previous estimate for the two-body self-energy correction, which is not accurate at $R_{i,j} \sim r_1$. Lastly, the elastic energy cost per unit volume [Eq. (13)] at metastable equilibrium is $E_{2D}^{(1)}/9\pi r_1^2 = (2/9)(\Delta r/r_1)^2 [c_\parallel^{(\mathrm{in})-1} + c_\perp^{(\mathrm{out})-1}]^{-1}$ in the marginally stable limit at $r_2^2 = 3 r_1^2$ (see Fig. 1). The strong dependence that it shows on the bulk compression modulus of the inclusion affects growth dynamics. This could be the root cause for the difference in length between BZO nanorods and BSO nanocolumns in YBCO.[5]

III. CRITICAL CURRENT BY TWO-DIMENSIONAL COLLECTIVE PINNING

We shall now determine the critical current of a thin film of superconducting YBCO threaded by nanorod inclusions along the crystalline c axis and subject to external magnetic field aligned along the same axis. Recall that the critical temperature in an optimally doped YBCO superconductor is primarily sensitive to *shear* strain in the a-b plane.[6] That fact coupled with the shear strain generated by a nanocolumn inclusion Eq. (5) results in a potential-energy landscape for vortex lines that can collectively pin the vortex lattice. In particular, the contribution of the vortex core to the vortex line tension is approximated by the fundamental energy scale per unit length $\varepsilon_0 = (\Phi_0/4\pi\lambda_L)^2$, where λ_L denotes the London penetration depth. The temperature dependence shown by the vortex line tension is therefore approximated by $\varepsilon_0(T) = \varepsilon_0(0)[1 - (T/T_{c0})]$ near the mean-field critical temperature T_{c0}. The potential-energy landscape experienced by a vortex line then has a contribution $\delta\varepsilon_1(\mathbf{r}) = \Sigma_\alpha \Sigma_\beta (\partial\varepsilon_0/\partial T_c)(\partial T_c/\partial \epsilon_{\alpha,\beta}) \epsilon_{\alpha,\beta}(\mathbf{r})$, where T_c is the true critical temperature and $\epsilon_{\alpha,\beta}$ is the symmetric strain tensor [Eq. (5)]. It results in a d-wave potential-energy landscape about the nanocolumn for a vortex core,

$$\delta\varepsilon_1(\mathbf{r}) = \varepsilon_p (r_{\mathrm{out}}/r)^2 \cos 2\phi, \tag{14}$$

with $\varepsilon_p = \varepsilon_0(0)(T/T_{c0}) T_c^{-1} [(\partial T_c/\partial \epsilon_{bb}) - (\partial T_c/\partial \epsilon_{aa})] B_0$. Here the ratio between T_{c0} and T_c is assumed to be constant. A rigid vortex line therefore experiences a force field,

$$\mathbf{f}_1(\mathbf{r}) = f_p (r_{\mathrm{out}}/r)^3 (\hat{\mathbf{r}} \cos 2\phi + \hat{\boldsymbol{\phi}} \sin 2\phi), \tag{15}$$

due to the strain generated by a single nanocolumn inclusion, where $f_p = 2\varepsilon_p/r_{\mathrm{out}}$ is the maximum force per unit length.

The above pinning/antipinning force [Eq. (15)] is long range. However the presence of an extended field of nanocolumns can cut the range off (see Fig. 2). Such forces are added within the present elastic approximation [Eq. (8)]: $\mathbf{f}(\mathbf{r}) = \Sigma_i \mathbf{f}_1(\mathbf{r} - \mathbf{R}_i)$. The d-wave nature of each isolated force

field [Eq. (15)] implies a null net force on average. A characteristic fluctuation of the force over the YBCO matrix remains: $\overline{f^2}=n_\phi \int' d^2r|\mathbf{f}_1(\mathbf{r})|^2=\frac{1}{2}(\pi r_{\text{out}}^2 n_\phi)f_p^2$, where integration (prime) is restricted to the YBCO matrix. Matching $\overline{f^2}$ with $|\mathbf{f}_1(\mathbf{r})|^2$ yields an effective range for each pinning/antipinning center $r_p=(2/\pi n_\phi)^{1/6}r_{\text{out}}^{2/3}$.

The *d*-wave potential [Eq. (14)] that acts on rigid vortex lines in the vicinity of the phase boundaries between the nanocolumn inclusions and the YBCO matrix has zero angle average. It therefore cannot pin down a vortex line in isolation. However previous work by one of the authors and Maley[7] implies that many of them collectively pin the Abrikosov vortex lattice. A hexatic Bose glass state can exist at low temperature.[8] It is a vortex lattice threaded by isolated lines of edge dislocations in parallel to the relatively weak correlated pinning/antipinning centers. Plastic creep of the vortex lattice associated with glide by such edge dislocations limits the critical current,[7] which is given by $j_c B/c \sim n_p f_p^2/c_{66}b$. Here n_p denotes the density of vortex lines pinned by the nanocolumns, $c_{66}=(\Phi_0/8\pi\lambda_L)^2 n_B$ is the elastic shear modulus of the pristine vortex lattice at a density n_B of vortex lines,[10] and b denotes the magnitude of the Burgers vector associated with the edge dislocations that thread the vortex lattice. The *d*-wave nature of the pinning/antipinning center [Eq. (14)] also implies that its occupation is purely random. The density of vortex lines that they collectively pin is then equal to $n_p=(\sigma_p n_B)n_\phi$, where $\sigma_p=\pi(r_p^2-r_{\text{out}}^2)$ is the effective cross-sectional area of a pinning/antipinning center (see Fig. 2). The critical current density therefore obeys a *pure* inverse square-root power law with magnetic field, $j_c \propto B^{-1/2}$. Taking the values of $\partial T_c/\partial \epsilon_{aa}=230$ K and $\partial T_c/\partial \epsilon_{bb}=-220$ K for the strain derivatives of T_c in optimally doped YBCO (Ref. 6) can result in a pinning efficiency, $|f_p|\xi/\varepsilon_0$, of 93% at liquid nitrogen temperature.

IV. DISCUSSION AND CONCLUSIONS

We have found that the growth of nanorod inclusions in YBCO films is very likely driven by weak metastability shown by the elastic energy of epitaxial layers. We also have pointed out how the sensitivity of the critical temperature in optimally doped YBCO to pure shear strain inside of the *a*-*b* plane[6] results in an effective collective pinning center for the Abrikosov vortex lattice at the phase boundary between the nanorod inclusion and the YBCO matrix.

However the lattice mismatch along the *c* axis between the nanorod inclusion and YBCO has so far been neglected. YBCO has a unit cell that can be divided into a stack of three cubes along the *c* axis, each with a lattice constant $c_{\text{out}}/3=3.9$ Å. The strain that results at the phase boundary with a BZO nanorod or with a BSO nanocolumn, both of which are cubic with lattice constants $a_{\text{in}}=4.2$ Å and 4.1 Å, respectively, can be relieved by introducing partial misfit dislocations accompanied by stacking faults in the YBCO matrix.[9] The predicted spacing between such stacking faults, $c_{\text{Moire}}=[(3/c_{\text{out}})-a_{\text{in}}^{-1}]^{-1}$, is then equal to 5 nm for BZO nanorods and 8 nm for BSO nanocolumns (cf. Ref. 5). Since their effect on the previous elasticity analysis can be accounted for by renormalized elastic moduli for the YBCO matrix, we believe that our conclusions remain unchanged in their presence.

ACKNOWLEDGMENTS

The authors thank George Levin for the discussions. This work was supported in part by the U.S. Air Force Office of Scientific Research under Grant No. FA9550-06-1-0479.

APPENDIX: SURFACE INTEGRALS

Equation (9) gives the surface integral that determines the three-body elastic interaction among nanocolumn inclusions. Integration by parts combined with $\nabla^2\mathbf{u}_\perp=0$ yields that it is symmetric with respect to the latter: $I_{i,j,k}=I_{i,k,j}$. In the case that $i=j$, it reduces to the angular integral,

$$I_{i,i,k}=\frac{1}{2}r_{\text{out}}^2 B_0^2\int_0^{2\pi} d\phi\left(\frac{R_{i,k}^2-r_{\text{out}}^2}{r_{i,k}^2}-1\right), \tag{A1}$$

where $r_{i,k}^2=r_{\text{out}}^2+R_{i,k}^2+2r_{\text{out}}R_{i,k}\cos(\phi-\phi_k)$. Here, ϕ_k denotes the orientation of the vector $\mathbf{R}_{i,k}=\mathbf{R}_i-\mathbf{R}_k$. After making the change of variables $z=e^{i\phi}$, application of Cauchy's theorem yields that the integral vanishes: $I_{i,i,k}=0$. In the case that $i\neq j$ and $i\neq k$, the surface integral Eq. (9) reduces to

$$I_{i,j,k}=\frac{1}{4}r_{\text{out}}^4 B_0^2\int_0^{2\pi} d\phi\left[\frac{(R_{i,j}^2-r_{\text{out}}^2)}{r_{i,j}^4}-\frac{1}{r_{i,k}^2}+\frac{R_{j,k}^2}{r_{i,j}^2 r_{i,k}^2}-\frac{(R_{i,j}^2-r_{\text{out}}^2)R_{j,k}^2}{r_{i,j}^4 r_{i,k}^2}+(j\leftrightarrow k)\right]. \tag{A2}$$

Repeating the previous steps results in a closed-form expression with a large number of terms. Symbolic manipulation programs then help reduce these to the result in Eq. (10).

[1] S. R. Foltyn, L. Civale, J. L. MacManus-Driscoll, Q. X. Jia, B. Maiorov, H. Wang, and M. Maley, Nat. Mater. **6**, 631 (2007).
[2] J. L. MacManus-Driscoll, S. R. Foltyn, Q. X. Jia, H. Wang, A. Serquis, L. Civale, B. Maiorov, M. E. Hawley, M. P. Maley, and D. E. Peterson, Nat. Mater. **3**, 439 (2004).
[3] A. Goyal, S. Kang, K. J. Leonard, P. M. Martin, A. A. Gapud, M. Varela, M. Paranthaman, A. O. Ijaduola, E. D. Specht, J. R. Thompson, D. K. Christen, S. J. Pennycook, and F. A. List, Supercond. Sci. Technol. **18**, 1533 (2005).
[4] C. V. Varanasi, J. Burke, L. Brunke, H. Wang, M. Sumption, and P. N. Barnes, J. Appl. Phys. **102**, 063909 (2007).
[5] P. Mele, K. Matsumoto, T. Horide, A. Ichinose, M. Mukaida, Y. Yoshida, S. Horii, and R. Kita, Supercond. Sci. Technol. **21**, 032002 (2008).
[6] U. Welp, M. Grimsditch, S. Fleshler, W. Nessler, J. Downey, G. W. Crabtree, and J. Guimpel, Phys. Rev. Lett. **69**, 2130 (1992).
[7] J. P. Rodriguez and M. P. Maley, Phys. Rev. B **73**, 094502 (2006).
[8] J. P. Rodriguez, Phys. Rev. B **76**, 224502 (2007).
[9] D. Hull and D. J. Bacon, *Introduction to Dislocations*, 3rd ed. (Pergamon, Oxford, 1984).
[10] E. H. Brandt, J. Low Temp. Phys. **26**, 735 (1977).